Journal of Molecular Catalysis, 54 (1989) 389 - 405

THE HIGHLY DISPERSED METAL STATE — PHYSICAL AND CHEMICAL PROPERTIES

H. MÜLLER, C. OPITZ

Department of Chemistry, Friedrich-Schiller-University Jena, 6900 Jena (G.D.R.)

and L. SKALA

Department of Chemical Physics, Charles-University Prague, 121 16 Prague (Czechoslovakia)

Summary

The region of highly dispersed metals is very interesting not only from a theoretical point of view but also in the field of practical catalysis.

Only quantum chemistry is able by means of an analytic cluster model (ACM) to calculate the properties $G(N)$ of metal clusters Me_N with arbitrary size ($N = 1, 2, 3, \ldots, \infty$). Because of very quick convergence of its asymptotical expansion, we can use very simple equations such as

$$G(N) = c_0 + c_{-1}/N^{1/3} \quad (1)$$

By fitting physically the coefficients c_i, eqn. (1) can be used as a rule of thumb to describe and predict size effects on various properties of small metallic particles. We have checked successfully the validity of eqn. (1) for a broad variety of properties of the highly dispersed metal state, such as electronic, geometric, thermodynamic, kinetic, optical, electrical and magnetic properties. In general, these size effects are responsible for the special catalytic behaviour of small metallic particles.

Introduction: the highly dispersed state of matter

Between the well-established microscopic domain of atoms and molecules mainly ruled by quantum chemistry and the macroscopic domain of condensed matter, governed by solid state physics, there is an intermediate region, dealing with properties of small particles or clusters, which are neither quite microscopic nor quite macroscopic (Fig. 1). This mesoscopic region of highly dispersed matter is very interesting, not only from a scientific point of view [1 - 4] ("the fifth state of matter" [5]), but also from a technological one [6] (catalysis, micro-electronics, high-tech ceramics etc.). Figure 1 shows that there are two possibilities of theoretical description within this mesoscopic region, starting: (i) from quantum chemistry via 'giant molecules' or (ii) from solid state physics via 'small solids'.

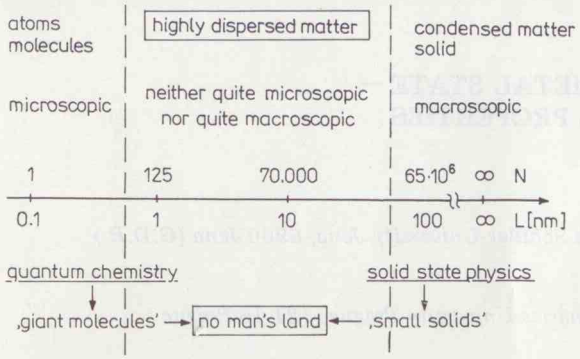

Fig. 1. Position of the highly dispersed state of matter within the conventional range of matter (*cf.* chapter 1.)

The main problem in this respect is the fact that giant molecules are much smaller than small solids, therefore we have from a theoretical point of view a 'no man's land' in this important region, that is, no adequate tools have been developed up to now.

The unique position of the analytic cluster model (ACM)

If we try to enter no man's land from the left-hand side (Fig. 2) in order to calculate a certain property G(N) as a function of particle size N ($N \sim$ number of atoms within the metallic particle Me_N), after a short distance $N \rightarrow N_{crit}$, all conventional quantum chemical approximation methods will fail (more sophisticated methods earlier, semi-empirical methods later); moreover, we have a very similar situation if we try to use the physical approach from the right hand side.

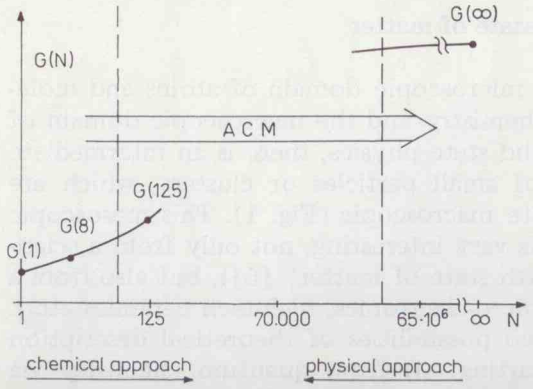

Fig. 2. The unique position of analytic cluster model (ACM) (*cf.* text.)

In this situation the question arises, how to investigate the fur development of size effect on property G if one goes from a single atom critical cluster $(Me_N)_{crit}$ to a bulk solid. The answer is unambiguous: the only one important exception, namely the ACM [7 - 13]. Only in this mo is any restriction concerning the number N of atoms removed complet The breakthrough concerning N must be paid for partly by the shortcomi of this method.

If we combine the most simple quantum chemical methods (HM FEM) with N-atom clusters characterized by specific regular boundaries, will have the rare possibility to solve the Schrödinger equation for cluster in an analytical manner, *i.e.* we will get closed formulas for ei values and eigen functions in dependence on N. Therefore, using ACM are able to calculate the properties of clusters with an arbitrary size [9, 12

Analytical calculation of a certain property G(N): an example [9]

We take as an example the calculation of the condensation ene $\Delta E(N)$ (= G(N)):

$$Me_N + Me \longrightarrow Me_{N+1};\ \Delta E(N)$$

at the one-dimensional solid in the framework of free electron model (FE In this case we are able to derive with paper and pencil eqn. (3) [9]:

$$\Delta E(N) = 0.361 + 1/4(N^3 + 47N^2/12 + 29N/6 + 93/48)(N^2 + 2N + 3/4)^{-2}$$

The larger N, the better the asymptotical expansion of $\Delta E(N)$ converges:

$$\Delta E(N) = 0.361 + 0.250/N - 0.0208/N^2 - 0.0834/N^3 + \ldots$$

If N is large enough, we can neglect all further terms and get the simple eq (5):

$$\Delta E(N) \approx 0.361 + 0.250/N$$

If we calculate the error F (%) which arises if we substitute the f eqn. (3) by the approximate eqn. (5), we get the interesting result which summarized in Table 1, that eqn. (5) also converges sufficiently for sm values of N.

TABLE 1

Error F (%) of ΔE calculated by the approximate eqn. (5) in comparison with the exa values of eqn. (3)

N	1	3	5	7	9	11
F (%)	7.4	0.8	0.3	0.2	0.15	0.1

Higher dimensional clusters lead to the more general expansion [14]

$$G(N) = c_0 + c_{-1}/N^{1/d} + c_{-2}/N^{2/d} + \ldots \quad (6)$$

$$G(N) \approx c_0 + c_{-1}/N^{1/d}; \quad (7)$$

where d denotes the dimension of the cluster. Equations (4) and (5) are special cases of eqns. (6) and (7) for $d = 1$.

It is convenient for larger clusters to convert N into the radius R of the particle; for this conversion we only need the mass density ρ. For three-dimensional clusters Me_N we use the following two asymptotical expansions:

$$G(N) = c_0 + c_{-1}/N^{1/3} + \ldots \quad (8)$$

$$G(R) = c_0 + k_{-1}/R + \ldots; \quad k_{-1} = c_{-1}(3M/4\pi N_A \rho)^{-1/3} \quad (9)$$

Physical parameterization of the asymptotical expansion of G(N)

Now we try to subdivide the main result of ACM (eqns. (8) and (9)) which is influenced by the shortcomings of the quantum chemical approximation into two parts:

(i) the first part caused by the cluster topology (and therefore a useful part), mainly given by the mathematical shape of the expansion, and
(ii) the second part caused by quantum chemical approximation (and therefore a defective part), mainly given by the numerical values of the expansion coefficients.

In order to obtain more reasonable results, we substitute the quantum chemical calculation of the expansion coefficients by its physical parameterization [15]:

— If we go to infinite clusters:

$$\lim_{N \to \infty} G(N) = \lim_{R \to \infty} G(R) = c_0 = G(\infty) \quad (10)$$

the physical meaning of c_0 becomes clear; c_0 is equal to the bulk value of the property G.

— If we consider a cluster containing n atoms:

$$\lim_{N \to n} G(N) = G(\infty) + c_{-1}(n)/n^{1/3} = G(n) \qquad n = 1, 2, \ldots \quad (11)$$

$$\lim_{R \to r_n} G(R) = G(\infty) + k_{-1}(n)/r_n = G(r_n)$$

we can find the physical meaning of the second coefficients $c_{-1}(n)$, $k_{-1}(n)$ in a similar way.

ACM — simple interpolation formulas

If we fit physically the first two expansion coefficients (eqns. (10) and (11)) and neglect all higher terms, we get simple interpolation formulas [15]:

$$G(N) = c_0 + c_{-1}/N^{1/3} \quad (12a, b)$$

$$G(R) = c_0 + k_{-1}/R$$

$$c_0 = G(\infty)$$

$$c_{-1} = c_{-1}(n) = [G(n) - G(\infty)]n^{1/3} \quad (13)$$

$$k_{-1} = k_{-1}(n) = [G(r_n) - G(\infty)]r_n \qquad n = 1, 2, \ldots$$

which can be used as rules of thumb to describe and predict size effects. (Please note that therefore a least square fit of experimental data is not our goal, although in a number of figures we would get better results in the region, defined by experimental data).

For practical use of these interpolation formulas (eqns. (12a, b)) in describing or predicting the size dependence of a certain property G(N), G(R), we only need two pieces of information (eqn. (13)):

(i) the bulk value G(∞), for many properties tabulated in the literature,
(ii) the value G(n)(G(r_n)) of a cluster containing n atoms (which is characterized by radius r_n); in general, these values G(n)(G(r_n)) must be measured or calculated at the cluster Me_n.

That means we only need a single measurement or a single calculation in order to get qualitative information as to the whole size dependence of the property G under consideration.

Of course we can use further terms in eqns. (8) and (9), at least the quadratic terms:

$$G(N) = c_0 + c_{-1}/N^{1/3} + c_{-2}/N^{2/3} \quad (12c, d)$$

$$G(R) = c_0 + k_{-1}/R + k_{-2}/R^2,$$

although experimental data and our experience show that $N^{-1/3}$ (R^{-1}) is the leading term. Using eqns. (12c, d) we are able to describe not only monotonic functions G (as in the case of eqns. (12a, b)) but stationary points too (minima, maxima). With respect to experimental data, much more important is the case, where function G exhibits gerade symmetry $c_{-(2n+1)} = 0$ ($k_{-(2n+1)} = 0$). In this special case $c_{-2}/N^{2/3}(k_{-2}/R^2)$ becomes the leading term and we get a faster convergence. (In this sense, *e.g.* $a^{Al}(R)$ in Fig. 6, *vide infra*, could be described more reasonably). In every case we lost the simplicity of our interpolation formulas eqns. (12a, b), because the physical parameterization of eqns. (12c, d) requires further information.

Verification of the interpolation formulas (eqns. (10a, b)

We have verified successfully the validity of our rules of thumb for a broad variety of about 40 various properties [15 - 17]. The next Figures (3 - 15) give a dozen examples. Many of these properties contribute considerably to a better understanding of the catalytic behaviour of small metallic particles.

Electronic properties

In this chapter we discuss the ionization potentials of potassium clusters, the polarizability of sodium clusters and the binding energy per atom of lithium clusters.

Ionization potential IP of metal clusters Me_N

The first example should be given in more detail. Figure 3 shows the IP of potassium clusters K_N as a function of the number N of atoms: $IP^K(N)$. Full circles represent experimental data given by Knight *et al.* [18], the dashed line corresponds with the bulk value, and the solid line shows the application of our simple asymptotical expansion (eqn. (15a)) which interpolates very well the experimental data. (With respect to ACM, it is easily understood that our simple interpolation formula cannot describe the well-known oscillations and steps in $IP^{Me}(N)$, connected with electronic shell structure.) In this case, physical parameterization:

$G(\infty) = IP^K(\infty) = \Phi^K{}_{bulk} \sim$ work function of potassium metal,

$G(1) = IP^K(1) = IP^K \sim$ ionization potential of potassium atom

is very convenient, because both values ($G(\infty)$, $G(1)$) are not only well-known for potassium [18]:

$\Phi^K{}_{bulk} = 2.3$ eV, $IP^K = 4.34$ eV

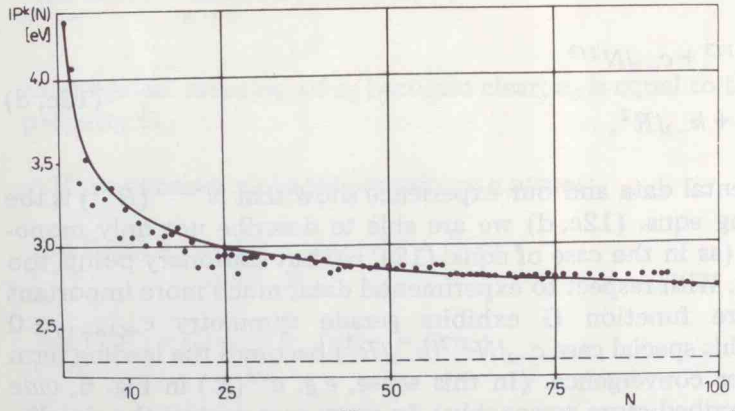

Fig. 3. Ionization potential $IP^K(N)$ of potassium clusters K_N as a function of cluster size N. (•) Experimental data reported by Knight *et al.* [18], (———) theoretical description by eqn. (15a) (ACM), (— — —) bulk value (= work function).

but for nearly all metals of the Periodic Table (*e.g.* [24]). Therefore we can predict the size effect on IP for clusters of nearly all metals:

$$IP^{Me}(N) = \Phi^{Me}{}_{bulk} + (IP^{Me} - \Phi^{Me}{}_{bulk})/N^{1/3}$$
$$IP^{Me}(R) = \Phi^{Me}{}_{bulk} + (4\pi N_A \rho^{Me}/3M)^{-1/3}(IP^{Me} - \Phi^{Me}{}_{bulk})/R \quad (14a, b)$$

In application to K clusters, eqns. (14a, b) read:

$$IP^K(N) = 2.3 + 2.04/N^{1/3} \text{ eV}$$
$$IP^K(R) = 2.3 + 5.35/R\ [\text{Å}] \text{ eV} \quad (15a, b)$$

If we define a reduced ionization potential IP_{red} of metal clusters:

$$IP^{Me}{}_{red}(N) = IP^{Me}(N)/\Phi^{Me}{}_{bulk} \quad (16)$$

and take into consideration that related metals characterized by mean values

$$\overline{(IP^{Me}/\Phi^{Me}{}_{bulk})}^{\{Me_i\}} = k + 1;\ k = \text{const.};\ Me \in \{Me_i\} \quad (17)$$

have only very small deviations, it becomes clear that various but related metals exhibit the same general size effect on this ionization potential

$$IP^{Me}{}_{red}(N) = 1 + k/N^{1/3};\ k = \text{const.},\ Me \in \{Me_i\} \quad (18)$$

As an example, we obtain for the alkali metals Me(Ia)

$$\overline{(IP^{Me}/\Phi^{Me}{}_{bulk})}^{\{Me(Ia)\}} = 1.89 \pm 0.05 \quad (19)$$

and

$$IP^{Me}{}_{red}(N) = 1 + 0.887/N^{1/3};\ Me \in \{Me(Ia)\} \quad (20)$$

in agreement with experimental data [18, 19].

As a result of classical image-potential theory, one obtains the size dependence of the work function or ionization potential of small metallic spheres on radius R [20, 21]:

$$IP^{Me}{}_{class}(R) = \Phi^{Me}{}_{bulk} + (3e^2/8)/R \quad (21a)$$

The reason is that the image-potential for a metallic sphere differs considerably from that of a plane. For potassium clusters, eqn. (21a) reads:

$$IP^K{}_{class}(R) = 2.3 + 5.40/R\ [\text{Å}] \text{ eV}. \quad (21b)$$

It is well known that eqn. (21) is valid only within a classical region of R ($R > R_{crit}$). But sometimes eqn. (21) is used successfully to interpret experimental data measured on clusters down to only a few atoms [20 - 23]. It is amazing that such a classical model should give an at all useful correlation at these small dimensions, but only at first glance. It is obvious that only the quantum chemically derived eqn. (15b) can be applied in this microscopic region ($R < R_{crit}$); please note that both equations (15b) and (21b) are very similar. Successful application of eqn. (21b) down to the

microscopic region means nothing else than application of eqn. (15b)! All further examples discussed in this paper will be summarized more concisely.

Polarizability α of alkali clusters

Molecular beam deflection measurements of static electric polarizability per atom, α/N, are reported by Knight *et al.* [25] for sodium clusters up to $N = 40$ and potassium clusters up to $N = 20$. We take as an example Na_N clusters. The quantity α/N decreases from the atomic polarizability to approximately 150% of the bulk value at $N = 40$ (Fig. 4).

Our interpolation formula:

$$\alpha_r^{Na}(N) = \alpha^{Na}(N)/N\alpha^{Na}(1) = 0.39 + 0.61/N^{1/3} \qquad (22)$$

(Parameterization: $\alpha_r(\infty) = 0.39$; $\alpha_r(1) = 1$)

reflects qualitatively the size dependence of $\alpha^{Na}(N)$.

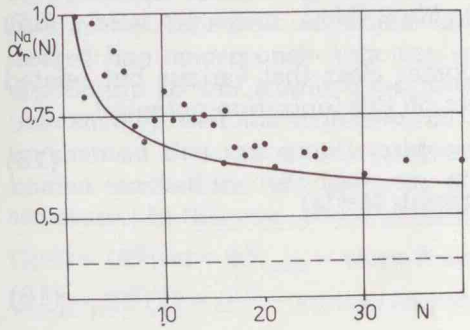

Fig. 4. Polarizability $\alpha^{Na}(N)$ of sodium clusters Na_N as a function of cluster size N. (•) Experimental data reported by Knight *et al.* [25], (——) theoretical description by eqn. (22) (ACM), (— — —) bulk value.

Binding energy per atom (BE) of metal clusters

The physical parameterization of our asymptotical expansion is very simple in the case of BE:

$BE(\infty) = BE_{bulk}$ ~ binding energy per atom of bulk metal

$BE(2) = 0.5\ D_e$, D_e ~ binding energy of metallic dimer Me_2.

Again, both values are well known for a large number of metals and therefore we can predict size effect on BE for many metal clusters:

$$BE^{Me}(N) = BE^{Me}{}_{bulk} + 2^{1/3}(0.5\ D^{Me}{}_e - BE^{Me}{}_{bulk})/N^{1/3} \qquad (23a, b)$$

$$BE^{Me}(R) = BE^{Me}{}_{bulk} + (2\pi N_A \rho^{Me}/3M)^{-1/3}(0.5\ D_e - BE^{Me}{}_{bulk})/R$$

There are no experimental data available, but we can verify successfully eqn. (23) by means of quantum chemically calculated (CNDO) data for Li_N clusters by Skala [26] ($D_e{}^{Li} = 1.05$ eV, $BE^{Li}{}_{bulk} = 2.01$ eV) (Fig. 5):

$$BE^{Li}{}_{CNDO}(N) = 2.01 - 1.87/N^{1/3}\ \text{eV} \qquad (24)$$

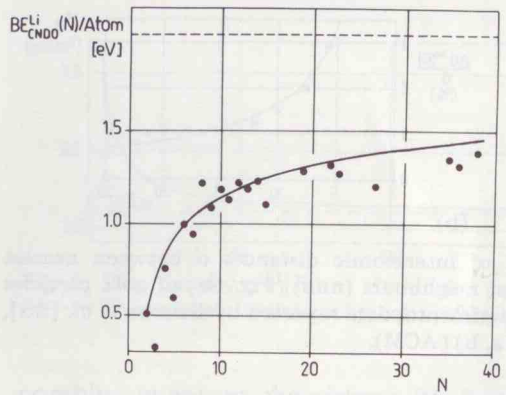

Fig. 5. Binding energy per atom $BE^{Li}{}_{CNDO}(N)$ of lithium clusters Li_N as a function of cluster size. (•) Quantum chemically calculated (CNDO) data reported by Skala [26], (——) theoretical description by eqn. (24) (ACM), (— — —) bulk value.

Geometrical properties

We now discuss the lattice parameter of Al particles and nearest neighbour and next nearest neighbour distances in Au particles.

Lattice parameter a of Al particles

Nepijko *et al.* [27] have measured lattice parameter of Al particles a^{Al} with radii between 25 and 150 Å (electron microscope and moiré fringe technique). Figure 6 represents the result concerning the decrease in lattice parameter a^{Al} with decreasing particle size R. Included in Fig. 6 is the qualitative description of this size dependence by means of our interpolation formula:

$$a^{Al}(R) = 4.049 - 2.01/R[\text{Å}] \quad \text{Å} \qquad (25)$$

(Parameterization: $a^{Al}(\infty) = 4.049$ Å, a^{Al} (3.24 Å) = 3.987 Å)

which fits satisfactorily the experimental data.

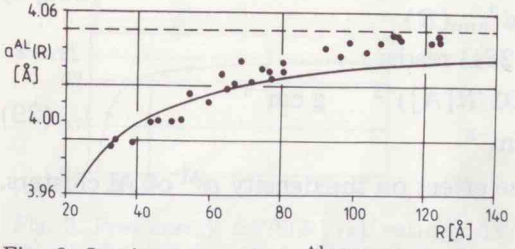

Fig. 6. Lattice parameter $a^{Al}(R)$ of aluminium particles Al(R) as a function of cluster size R. (•) Experimental data reported by Nepijko *et al.* [27], (——) theoretical description by eqn. (25) (ACM), (— — —) bulk value.

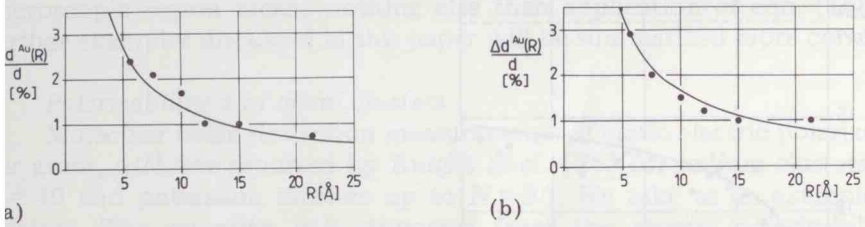

Fig. 7. Relative contraction $\Delta d^{Au}(R)/d$ of interatomic distances d between nearest neighbours (nn) (Fig. 5a) and next nearest neighbours (nnn) (Fig. 5b) of gold particles $Au(R)$ as a function of cluster size. (●) Experimental data reported by Balerna *et al.* [28], (——) theoretical description by eqns. (27a, b) (ACM).

Lattice distances d in Au clusters

Balerna *et al.* [28] reported on structural investigation using EXAFS spectra recorded on Au metal clusters, whose average diameters ranged from 1 to 50 Å. They found contraction of interatomic distances d between nearest neighbours (nn) and next nearest neighbours (nnn) (Fig. 7). Our rules of thumb:

$$d^{Au}{}_{nn}(R) = 2.88 - 0.385/R[\text{Å}] \quad \text{Å}$$
$$d^{Au}{}_{nnn}(R) = 4.07 - 0.66/R[\text{Å}] \quad \text{Å} \qquad (26a, b)$$

Parameterization: $d_{nn}(\infty) = 2.88$ Å, $d_{nn}(5.5\ \text{Å}) = 2.81$ Å
$d_{nnn}(\infty) = 4.07$ Å, $d_{nnn}(5.5\ \text{Å}) = 3.95$ Å)

or the corresponding contraction percentage $\Delta d^{Au}(R)/d$ $(= [d(\infty) - d(R)]/d(\infty))$

$$\Delta d^{Au}{}_{nn}(R)/d = 13.4/R[\text{Å}]$$
$$\Delta d^{Au}{}_{nnn}(R)/d = 16.2/R[\text{Å}] \qquad (27a, b)$$

fit very well the experimental data.

Density ρ of metal clusters

If we consider the results from the above sections, for obvious reasons we can predict the size effect on density ρ of clusters (from atoms of mass $m = M/N_A$) using the size dependence of lattice parameters a^{Me}, d^{Me}:

$$\rho_{fcc}(R) = 4M/N_A a^3(R) = 2^{1/2} M/N_A d^3{}_{nn}(R)$$
$$\rho_{bcc}(R) = 2M/N_A a^3(R) = 3^{3/2} M/N_A d^3{}_{nnn}(R) \qquad (28a, b)$$

For example, for Al_N clusters eqn. (28a) reads:

$$\rho^{Al}(R) = 6.642\ M^{Al}[\text{g}]\ (4.049 - 2.01/R[\text{Å}])^{-3} \quad \text{g cm}^{-3}$$
$$\rho^{Al}(R) = (2.70 + 4.02/R[\text{Å}]) \quad \text{g cm}^{-3} \qquad (29)$$

Figure 8 illustrates this predicted size effect on the density ρ^{Al} of Al clusters.

Thermodynamic properties

With this chapter we reach phenomenological or macroscopic properties, respectively. To calculate these properties, strictly speaking, we had to

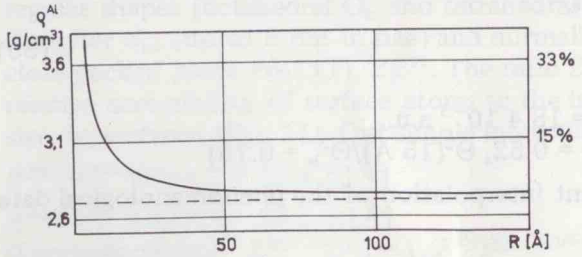

Fig. 8. Mass density $\rho^{Al}(R)$ of aluminium particles $Al(R)$ as a function of cluster size R. (——) Theoretical prediction by eqn. (29) (ACM), (— — —) bulk value.

combine quantum chemistry with further theories. Nevertheless, also in this case we use the asymptotical expansion from ACM to tentatively describe phenomenological size effects.

Free energy ΔF, entropy ΔS and Einstein temperature Θ of metal clusters

Hasegawa *et al.* [29] developed a microscopic theory in order to explain how the melting point in metallic small particles is dependent on size. In this connection they calculated various thermodynamic properties for Al, Pb, and Ag clusters whose radii range from 15 to 200 Å. As an example, Fig. 9a, b, c represents the calculated results as to Al particles (full circles): free energy $\Delta F(R) = F(R) - F(\infty)$, entropy $\Delta S(R) = S(R) - S(\infty)$, and Einstein temperature $\Theta^2(R)/\Theta^2{}_b$ ($\Theta_b \sim$ bulk value at the theoretical melting point). Solid lines in Fig. 9a, b, c correspond to our rules of thumb:

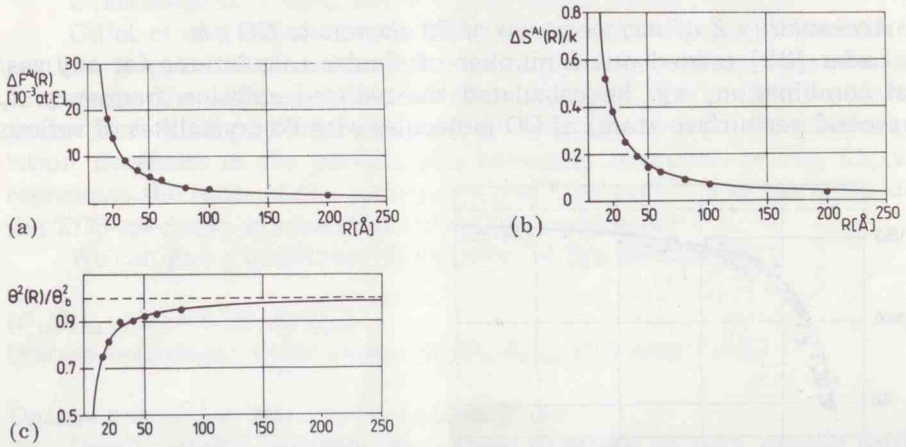

Fig. 9. Free energy $\Delta F^{Al}(R)$ (a), entropy $\Delta S^{Al}(R)$ (b) and Einstein temperature $\Theta^{Al}(R)$ (c) of aluminium particles $Al(R)$ as a function of cluster size R. (●) Calculated data reported by Hasegawa *et al.* [29], (——) theoretical description by eqn. (30) (ACM), (— — —) bulk value.

$$\Delta F^{Al}(R) = 0.276/R[\text{Å}] \quad \text{a.u.}$$
$$\Delta S^{Al}(R)/k = 7.83/R[\text{Å}] \qquad (30)$$
$$\Theta^2(R)/\Theta^2{}_b = 1 - 3.75/R[\text{Å}]$$

(Parameterization: $\Delta F(15\ \text{Å}) = 18.4\ 10^{-3}$ a.u.,
$\Delta S(15\ \text{Å})/k = 0.52$, $\Theta^2(15\ \text{Å})/\Theta^2{}_b = 0.75$)

which demonstrate an excellent interpolation of the phenomenological data given by Hasagawa *et al.* [29].

Melting temperature T_m of Au particles

The melting temperature T_m of small particles exhibits a remarkable size effect, because the decrease in T_m amounts to several hundred degrees. This thermodynamic size effect has been predicted in terms of phenomenological thermodynamics as early as in 1909 by Powlow [30]. But the experimental proof was first obtained in 1954 [31].

Figure 10 presents experimental data of the melting points of small Au particles [32], measured by a scanning electron-diffraction technique; this method was applied to particles having radii down to 10 Å. The solid line in Fig. 10 corresponds to our asymptotical expansion:

$$T^{Au}{}_m(R) = 1336.15 - 5543.65/R[\text{Å}] \quad \text{K} \qquad (31)$$

(Parameterization: $T_m(\infty) = 1336.15$ K, T_m (9.7 Å) = 764.64 K)

which gives again a reasonable description of this size dependence.

Kinetic properties

Among other things, we have selected for discussion accessibility and chemisorptional behaviour within the system carbon monoxide/palladium clusters.

Accessibility Z of surface atoms of Pd clusters to CO gas

Ladas [33] carried out a number of similar calculations for any gas/metal combination; *e.g.* he calculated the reduced collision frequency Z_r (per second per surface atom) of CO molecules with Pd crystallites of various

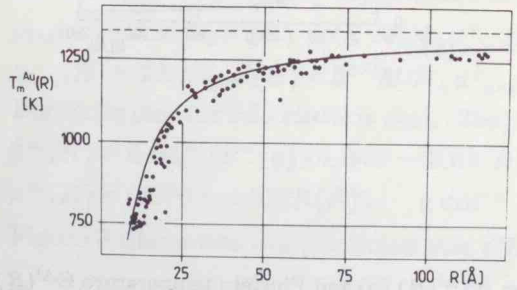

Fig. 10. Melting temperature $T^{Au}{}_m(R)$ of gold particles Au(R) as a function of cluster size R. (●) Experimental data reported by Buffat *et al.* [32], (——) theoretical description by eqn. (31) (ACM), (— — —) bulk value.

regular shapes (octahedral O_h and tetrahedral T_d clusters) and varied average diameter d_{av} (up to 5 nm in size) and normalized with respect to that of the close-packed plane Pd(111), $Z_r{}^{111}$. The ratio $Z = Z_r/Z_r{}^{111}$ which describes the relative accessibility of surface atoms to the impinging gas exhibits a notable size dependence (Fig. 11). Our simple interpolation formulas:

$$Z^{Pd(T_d)/CO}(R) = 1 + 15.4/R[\text{Å}]$$
$$Z^{Pd(O_h)/CO}(R) = 1 + 13.2/R[\text{Å}] \qquad (32a, b)$$

(Parameterization: $Z^{Pd/CO}(\infty) = 1$, $Z^{Pd(T_d;O_h)/CO}(9.85\ \text{Å}) = 5.0; 4.42$)

give a qualitative description of these size effects and a certain separation of size and structure effects.

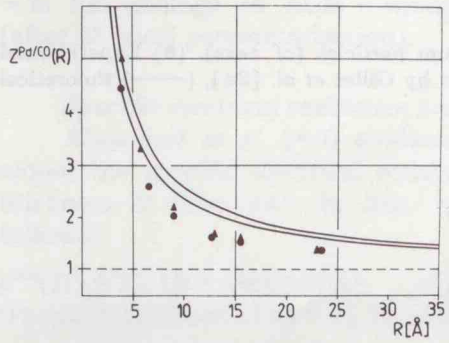

Fig. 11. Accessibility $Z^{Pd/CO}(R)$ of surface atoms of palladium particles Pd(R) to CO gas as a function of cluster size R. (▲●) Calculated data (▲ ~ tetrahedral, ● ~ octahedral) reported by Ladas [33], (——) theoretical description by eqns. (32a, b) (ACM), (— — —) bulk value.

Chemisorptional behaviour of small supported Pd particles

Gillet *et al.* [34] studied in detail CO chemisorption on well-defined Pd particles supported on mica. For our purpose we extract only the results concerning the thermal CO desorption spectra (TDS), which exhibit two peaks. Peak 1 fills first and saturates at about 3L exposure. Its relative population decreases as the particle size increases, as shown in Fig. 12, which represents the ratio of the area under the TDS peak 1 and the total area of the TDS spectrum at saturation *versus* the particle size.

We can give a qualitative description of this dependence:

$$(\theta_1/\theta_t)_{sat.}(R) = 0.38/R[\text{nm}] \qquad (33)$$

(Parameterization: 'bulk' value = 0, $(\theta_1/\theta_t)_{sat}$ (0.7 nm) = 0.51

Optical properties: Mie resonance absorption

Small metallic particles often show beautiful colours, usually different from the colours of the bulk metal. An explanation of this optical size effect (optical resonance absorption) was given again early in this century by Mie [35] in terms of classical electrodynamics.

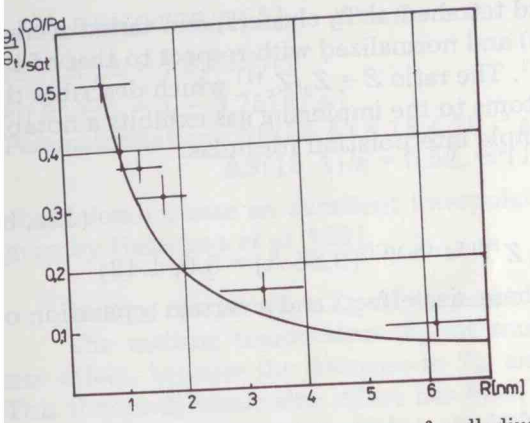

Fig. 12. Chemisorptional behaviour of palladium particles (*cf.* text). (●) Experimental data (thermal CO desorption spectra) reported by Gillet *et al.* [34], (——) theoretical description by eqn. (33) (ACM).

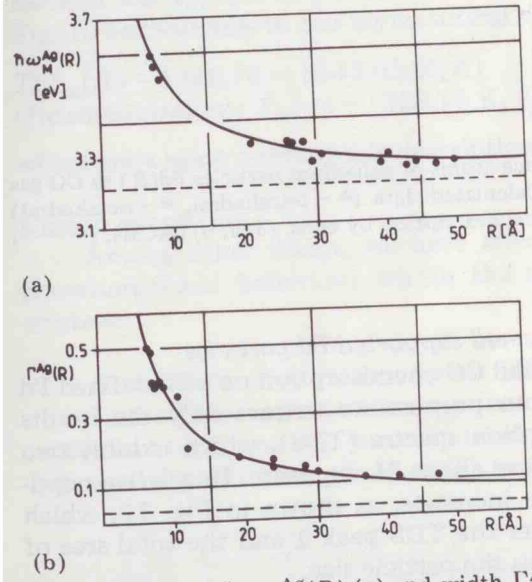

Fig. 13. Position $\hbar\omega_M{}^{Ag}(R)$ (a) and width $\Gamma^{Ag}(R)$ (b) of the optical resonance absorption peak (Mie absorption) of silver particles Ag(R) in argon matrix, as a function of cluster size R. (●) Experimental data reported by Bennemann *et al.* [36], (——) theoretical description by eqns. (34a, b) (ACM), (— — —) bulk value.

Figure 13 shows experimental results for the position $\hbar\omega_M$ and width Γ of the resonance absorption peak as a function of cluster radius R for Ag clusters in an Ar matrix, presented by Bennemann and Reindl [36].

Our rules of thumb

$$\hbar\omega_M{}^{Ag}(R) = 3.21 + 2.77/R[\text{Å}]\ \text{eV}$$
$$\Gamma^{Ag}(R) = 0.03 + 2.94/R[\text{Å}]\ \text{eV} \qquad (34a, b)$$

(Parameterization: $\hbar\omega_M(\infty) = 3.21$ eV, $\hbar\omega_M$ (7.3 Å) = 3.59 eV
$\Gamma(\infty) = 0.03$ eV, Γ (6.4 Å) = 0.49 eV)

again describe very successfully these size effects.

Electrical and magnetic properties

We discuss in the last chapter specific electrical resistance and the Hall coefficient of metallic films, because of completeness of groups of properties on the one hand and to show on the other hand that the analytical film model (AFM) [37 - 39] is also able to produce simple interpolation formulas — in full analogy to ACM — which again can be used as rules of thumb (after physical parameterization).

Specific electrical resistance ρ of Sn films

Abou-Saif *et al.* [40] studied experimentally (four-point probe technique) the specific electrical resistance of Sn films in dependence on film thickness D (Fig. 14). In this case, our interpolation formula reads as follows:

$$\rho^{Sn}(D) = 11.15 + 4900/D[\text{Å}] \quad \mu\Omega\,\text{cm} \qquad (35)$$

(Parameterization: $\rho(\infty) = 11.15\ \mu\Omega$ cm, ρ (315 Å) = 26.5 $\mu\Omega$ cm)

and describes well the entire size dependence of ρ^{Sn}.

Hall coefficient $R^K{}_f$ of K films

Figure 15 presents the Hall coefficient R_f as a function of thickness for potassium thin films; experimental data (at 90 K) were taken from [41, 42]. Our simple formula

$$R^K{}_f(D) = 42 + 565/D[\text{Å}] \quad 10^5\ \text{cm}^3\ \text{C}^{-1} \qquad (36)$$

interpolates qualitatively the experimental data.

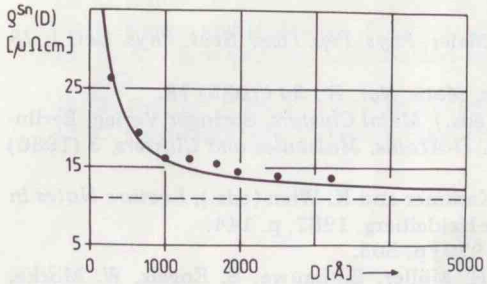

Fig. 14. Specific electrical resistance $\rho^{Sn}(D)$ of tin films Sn(D) as a function of film thickness D. (●) Experimental data reported by Abou-Saif *et al.* [40], (——) theoretical description by eqn. (35) (AFM), (— — —) bulk value.

Fig. 15. Hall coefficient $R^K_f(D)$ of potassium films K(D) as a function of film thickness D. (●) Experimental data reported by Crikler [41]/Govindaraj and Devanathan [42], (——) theoretical description by eqn. (36) (AFM), (— — —) bulk value.

Concluding remarks: rules of thumb for catalysts

The study of physical and chemical properties of small particles belonging to the mesoscopic region, *i.e.* that contain too many atoms to be a molecule, but not enough to be a solid, is difficult not only theoretically, but also experimentally. We have overcome this difficulty by using the unique but very simple ACM, which is able to describe size dependence of cluster properties G(N) in the whole region $N = 1, 2, \ldots, \infty$. As a consequence the results are strongly influenced by the shortcomings of the quantum chemical approximation. Nevertheless we obtained reasonable results (by physical parameterization of expansion coefficients): simple interpolation formulas which can be used as rules of thumb to describe and predict size effects of a broad variety of physical and chemical properties G(N).

We are actually convinced that these interpolation formulas can also be helpful in catalysis in order to estimate properties of small metallic particles of catalysts as a function of their cluster size.

References

1 J. A. A. J. Perenboom, P. Wyder and F. Meier, *Phys. Pep. (Rev. Sect. Phys. Lett.), 78* (1981) 173.
2 H. Müller, *Wiss. Z. Humboldt-Univ. Berlin, Math.-Nat. R., 34* (1985) 78.
3 Müller, in F. Traeger and G. zu Putlitz (eds.), *Metal Clusters*, Springer Verlag, Berlin-Heidelberg, 1986, p. 133; *idem, Z. Phys. D-Atoms, Molecules and Clusters, 3* (1986) 233.
4 L. Skala and H. Müller, in E. R. Hilf, F. Kammer and K. Wien (eds.), *Lecture Notes in Physics*, Vol. 269, Springer Verlag, Berlin-Heidelberg, 1987, p. 144.
5 G. D. Stein, *The Physics Teacher, Nov.* (1979) p. 503.
6 H.-G. Fritsche, P. Kadura, L. Künne, H. Müller, E. Bauwe, S. Engels, W. Mörke, G. Rasch, P. Birke, H. Spindler; M. Wilde, H. Lieske und J. Völter: *Z. Chem., 24* (1984) 169.
7 T. A. Hoffmann, *Acta Phys. Hung., 1* (1951) 1; *ibid., 2* (1952) 97.

8 R. P. Messmer, *Phys. Rev. B, 15* (1977) 1811.
9 H. Müller, *Z. Chem., 12* (1972) 475.
10 L. Skala, *Czech. J. Phys., B 27* (1977) 171.
11 O. Bilek and P. Kadura, *Phys. Stat. Sol. (b), 85* (1978) 225.
12 P. Kadura and L. Künne, *Phys. Stat. Sol. (b), 88* (1978) 537.
13 L. Künne, O. Bilek and L. Skala, *Czech. J. Phys., B 29* (1979) 1030.
14 L. Skala, *Phys. Stat. Sol. (b), 127* (1985) 567.
15 H. Müller, Ch. Opitz, K. Strickert and L. Skala, *Z. Phys. Chem. (Leipzig), 268* (1987) 625.
16 H. Müller, Ch. Opitz, S. Romanowski and L. Skala, *Phys. Stat. Sol. (b), 148* (1988) K 11.
17 H. Müller, C. Opitz and S. Romanowski, *Z. Phys. Chem. (Leipzig), 270* (1989) 33.
18 W. D. Knight, W. A. De Heer and W. A. Saunders, *Z. Phys. D-Atoms, Molecules and Clusters, 3* (1986) 109.
19 M. Kappes, M. Schär, P. Radi and E. Schumacher, *J. Chem. Phys., 84* (1986) 1863.
20 I. Smith, *J. Am. Inst. Aeronaut. Astronaut., 3* (1965) 648.
21 D. Wood, *Phys. Rev. Lett., 46* (1981) 749.
22 E. Schumacher, M. Kappes, K. Marti, P. Radi, M. Schär and B. Schmidhalter, *Ber. Bunsenges. Phys. Chem., 88* (1984) 220.
23 M. M. Kappes, *Chem. Rev., 88* (1988) 369.
24 R. C. Weast (ed.), *Handbook of Chemistry and Physics*, CRC Press, Boca Raton, FL, 1979/80.
25 W. D. Knight, K. Clemenger, W. A. De Heer and W. A. Sauders, *Phys. Rev., B 31* (1985) 2539.
26 L. Skala, *Phys. Stat. Sol. (b), 107* (1981) 351; *ibid., 109* (1982) 733; *ibid., 110* (1982) 299.
27 S. A. Napijko, E. Pippel and I. Woltersdorf, *Phys. Stat. Sol. (a), 61* (1980) 469.
28 A. Balerna, E. Bernieri, P. Picozzi, A. Reale, S. Santucci, E. Buratini and S. Mobilio, *Surf. Sci., 156* (1985) 206.
29 M. Hasegawa, K. Hoshimo and M. Watabe, *J. Phys. F-Metal Phys., 10* (1980) 619.
30 P. Powlow, *Z. Phys. Chem. (Leipzig), 65* (1909) 545.
31 M. Takagi, *J. Phys. Soc. Jpn., 9* (1954) 359.
32 Ph. Buffat and J.-P. Borel, *Phys. Rev., A 13* (1976) 2287.
33 S. Ladas, *Surf. Sci., 159* (1985) L 406; *ibid., 175* (1986) L 681.
34 E. Gillet, S. Channakhone, V. Matolin and M. Gillet, *Surf. Sci., 152/153* (1985) 603.
35 G. Mie, *Ann. Phys. (Leipzig), 25* (1908) 377.
36 K.-H. Bennemann and S. Reindl, *Ber. Bunsenges. Phys. Chem., 88* (1984) 276.
37 L. Künne and R. Berndt, *Wiss. Z. Friedrich-Schiller-Univ. Jena, Math.-Nat. R., 25* (1976) 757.
38 L. Künne, *Z. Phys. Chem. (Leipzig), 265* (1984) 745.
39 L. Künne and H. Müller, *Z. Chem., 26* (1986) 345.
40 E. A. Abou-Saif, A. A. Mohamed and M. G. El-Khodary, *Thin Solid Films, 94* (1982) 133.
41 W. Crikler, *Z. Phys., 147* (1957) 481.
42 G. Govindaraj and V. Devanathan, *Phys. Rev., B 32* (1985) 2628.